

Loop transducer matching for low insertion loss magnetostatic surface wave resonator

D. K. De

Citation: *Journal of Applied Physics* **64**, 5210 (1988); doi: 10.1063/1.342434

View online: <http://dx.doi.org/10.1063/1.342434>

View Table of Contents: <http://scitation.aip.org/content/aip/journal/jap/64/10?ver=pdfcov>

Published by the [AIP Publishing](#)

Articles you may be interested in

[Low-loss unidirectional transducer for high frequency surface acoustic wave devices](#)

J. Appl. Phys. **110**, 076103 (2011); 10.1063/1.3651617

[A new microwave ring resonator using guided magnetostatic surface waves](#)

J. Appl. Phys. **55**, 2521 (1984); 10.1063/1.333715

[Magnetostatic wave interdigital transducers](#)

J. Appl. Phys. **49**, 1797 (1978); 10.1063/1.324704

[Low Insertion Loss Microwave Ultrasonic Delay Device Using a ZnO Thin Film Transducer](#)

J. Appl. Phys. **40**, 4983 (1969); 10.1063/1.1657330

[Insertion Loss of Side Branch Resonators](#)

J. Acoust. Soc. Am. **28**, 149 (1956); 10.1121/1.1918057

The advertisement features a dark blue background with a film strip graphic on the left. The text is centered and reads: 'Not all AFMs are created equal' in orange, 'Asylum Research Cypher™ AFMs' in white, and 'There's no other AFM like Cypher' in orange. At the bottom, the website 'www.AsylumResearch.com/NoOtherAFMLikeIt' is listed in white, and the Oxford Instruments logo is in the bottom right corner with the tagline 'The Business of Science®'.

Not all AFMs are created equal

Asylum Research Cypher™ AFMs

There's no other AFM like Cypher

www.AsylumResearch.com/NoOtherAFMLikeIt

OXFORD
INSTRUMENTS
The Business of Science®

Loop transducer matching for low insertion loss magnetostatic surface wave resonator

D. K. De^{a)}

Department of Electrical Engineering, The University of Texas at Arlington, Arlington, Texas 76019

(Received 25 May 1988; accepted for publication 3 August 1988)

In this paper we describe the matching of a loop transducer to significantly reduce the insertion loss and to improve the off-resonance rejection of a magnetostatic surface wave resonator.

INTRODUCTION

Magnetostatic wave (MSW) devices¹⁻⁸ form the basis of a new class of emerging microwave analog signal processing devices. Among these devices, MSW resonators and the corresponding loop transducers can be fabricated using conventional UV photolithography. It provides broad frequency tunability (2–18 GHz) by an external magnetic field. The insertion loss is low, and the Q is moderate, whereas for acoustic wave resonators one needs submicron photolithography. Although Q is usually high the insertion loss is also very high at microwave frequencies. It is well known that yttrium iron garnet sphere resonators operate well at microwave frequencies but require tedious and expensive fabrication procedures. MSW techniques, however, provide a simpler means of obtaining very high Q resonators for MSW oscillator and complex filter functions. In an earlier paper⁹ I discussed the magnetostatic surface wave (MSSW) resonators in detail. In this paper I focus on how the matching of the loop transducer with MSSW resonators was done.

We initially prepared 3-mm-wide, 1-in-long MSSW resonators on epitaxially grown YIG films on GGG substrates by usual standard UV photolithography techniques. To drive these resonators in the 2–6 GHz region we fabricated microstrip loop transducers (see Fig. 1) (MSW wavelength was chosen to be $300\ \mu\text{m}$). The MSSW resonators are driven with structure A of Fig. 1 in flipped configuration on structure B. Although the resulting Q (quality factor) of the resonators driven by the said loop transducers were in the region 800–3000 in the frequency range 3–6 GHz, the corresponding insertion losses were very high (15–34 dB) when 3-mm-long microstrip loop transducers were used. Moreover, the 3-mm-wide resonators with 3-mm-long loop transducer combinations were not tunable beyond 4.5 GHz because of the occurrence of the uniform resonance mode with IL higher than the MSSW mode and very low Q . Using a 1-mm-wide resonator with a 1-mm-long microstrip loop transducer ($\lambda_{\text{MSW}} = 300\ \mu\text{m}$, separation between the loop microstrips is $150\ \mu\text{m}$, see Fig. 2) the insertion loss was reduced to 8–20 dB. The different resonator responses with both matched and unmatched transducers are shown in Tables I and II. In order to reduce the insertion loss further, it was necessary that a 1-mm-long microstrip loop transducer was matched to 50- Ω input-output load, at resonance. The matching sig-

nificantly improved the tunability over a very wide frequency range and the insertion losses and the off-resonance rejection of the resonators. (See Table II and Figs. 3 and 4.)

For matching, S_{11} parameters (both magnitude and phase) were determined using a HP network analyzer with the resonator I (see Tables I and II) at several frequencies over 3–6 GHz. Before measuring the S_{11} parameters, the S_{11} channel of the network analyzer was adjusted so that the S_{11} magnitude and phase were 1° and 180° , respectively, at each frequency in the range 3–6 GHz when a 1-mm transducer short was used alone. The transducer short was made by grounding at the input of the microstrips of an identical loop transducer. The resonator was then set at resonance at the same frequency and the S_{11} parameters were determined (thus the S_{11} parameters were determined with respect to the transducer short). S_{11} parameters were plotted on a Smith chart (see Fig. 5) and the primary matching design as followed as provided by Hewlett-Packard Application Note 154. As matching over an octave band of 3–6 GHz is difficult, we tried finally to optimize the matching through computer optimization of microwave passive and active circuits (COMPACT). The circuit which optimized the matching is shown in Fig. 2(a) (assuming it is built on $250\text{-}\mu\text{m}$ quartz substrates which have $\epsilon_r = 3.8$). The widths W_1 and W_2 of the transmission line microstrips AB and CD as obtained from COMPACT were 0.52 and 0.55 mm, respectively, and the corresponding lengths were 6 and 5 mm, respectively [see Figs. 2(a) and 2(b)]. The values of $L = 1.51\ \text{nH}$ and $C = 0.3\ \text{pF}$ [Fig. 2(a)] were also obtained from COMPACT. The optimized S_{11} parameters within 400–5850 MHz are also shown in Fig. 5. We were not concerned about optimization in the range 3–4 GHz, because the insertion loss at resonance was within 6–12 dB even with an unmatched 1-mm transducer.

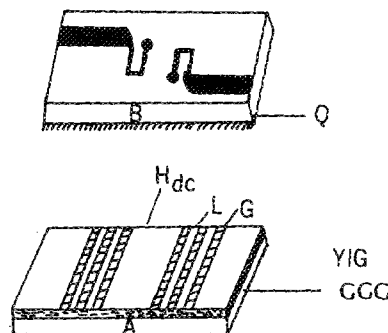


FIG. 1. A general schematic of a MSSW resonator with the corresponding loop transducer. The dimension of a typical resonator is $25\ \text{mm} \times 1\ \text{mm} \times 264\ \mu\text{m}$ ($14\text{-}\mu\text{m}$ YIG film on $250\text{-}\mu\text{m}$ GGG substrate).

^{a)} Present address: Radiology Department, The Bowman Gray School of Medicine, 300 S. Hawthorne Road, Winston Salem, NC 27103.

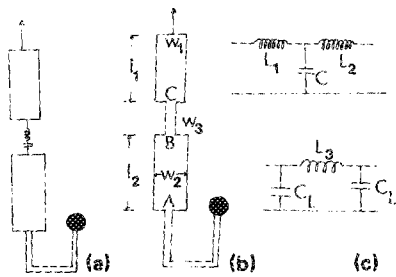


FIG. 2. (a) Lumped equivalent circuit of the input transmission lines obtained after matching through COMPACT using S_{11} parameters of the loop transducer in the range 3–6 GHz. The dimension of the loop microstrip of the transducer is 1 mm \times 50 μ m. This is designed for 300- μ m MSSW wavelength. Input and output transducers are separated by 2.4 mm. They are placed within the cavity of the resonator. (b) Microstrip equivalent circuit of the input transmission lines for the matched loop transducer. (c) Equivalent circuit of the inducer microstrip between A and C.

MICROSTRIP MATCHED CIRCUIT

In order to fabricate the above-mentioned computer optimized circuit of Fig. 2(a) on 250- μ m-thick quartz substrates in the form of microstrips only, it was necessary to utilize the inductance and capacitance of the microstrips so that the required inductance of $L = 1.51$ nH and the capacitance $C = 0.3$ pF could be introduced in the microstrips without the necessity of lumped components. The microstrip structure of Fig. 2(b) was found to be very convenient for photolithographic reproduction on quartz substrates. Its equivalent circuit is shown in Fig. 2(c). To calculate the required lengths l_i and the width W of the microstrip between B and C, the following points were taken into account:

(1) High impedance microstrip line ($Z_{OL} = 100 \Omega$) was used for inductance. The required length l_i and the W width of the microstrip line of the inductance 1.5 nH and capacitance of 0.3 pF [see Fig. 2(b)] were determined below.

(2) Discontinuity capacitance and inductance (at points A, B, and C) were utilized to provide the required L and C in the circuit as shown in Figs. 2(b) and 2(c). Figure

TABLE I. Physical characteristics of the resonators.

Resonator No.	Number of grooves	L (μ m)	G (± 6)	Separation between the arrays (mm)	Depth of the grooves	YIG thickness (μ m)
X1	40	65	80	3	1.1	15.3
X2	60	75	72	1.5	0.32	14.4
X6	55	3	0.4	16
K8	70	3.6	0.34	11.9
K2	65	70	76	3.0	0.42	13.9
K2'	65	70	76	3.0	0.62	13.9
I	70	72	72	3.6	0.7	7
X11	60	63	81	1.5	0.33	16

TABLE II. Summary of resonators response data.

Resonator No.	Aperature (mm)	Frequency (GHz)	Insertion loss (dB)	Optimized $Q \pm 50$	Resonance clearance (dB)
X1	1	3	8	300	8
		5	14	800	10
		6	19	1100	10
X3	1	3	17	650	7
		6	25	2000	6
		3	10	400	9
X6	1	6	19	1200	10
		3	13	400	7
		6	20	1250	8
X11	1	3	13	400	7
		6	20	1250	8
		6	20	1200	10
K8	1	3	11	500	8
		6	20	1700	9
		3	12	550	8
K2	1.5	6	20	1900	9
		3	8	550	9
		6	14	1500	15
I	1	3	8	650	8
		6	20	2000	10
		3	7	450	9
K2'	1.5	6	13	1300	15

2(c) is the equivalent circuit of the microstrip discontinuities.

The frequency ($f = 4.5$ GHz) in the following equations¹⁰ was chosen to be the center of the 3–6 GHz band:

$$\epsilon_{\text{eff}}(f) = \epsilon_r - \frac{\epsilon_r - \epsilon_{\text{eff}}}{[(1 + (h/Z_0)^{1.33}(0.43f^2 - 0.009f^3))]} \quad (1)$$

$$\epsilon_{\text{eff}}^C = \epsilon_r / \{0.96\epsilon_r + (0.109 - 0.004\epsilon_r)[\log(10 + Z_{0c}) - 1]\} \quad (2)$$

for $Z_{0c} < 50 \Omega$,

i.e., for capacitive microstrip and

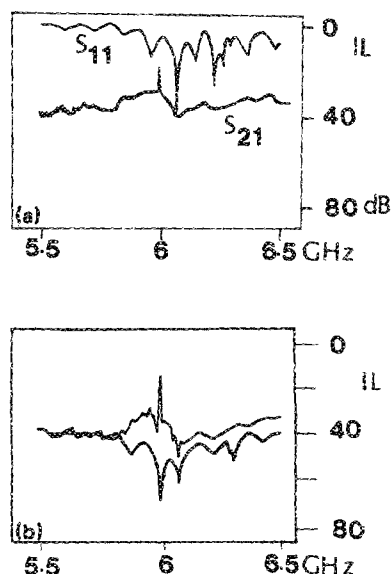


FIG. 3. (a) Resonator response at 6 GHz. 1-mm resonator K2 is used with a 1-mm matched transducer. It is seen that the S_{11} notch (lower curve) coincides with the S_{21} peak (upper) trace. Sweep range = 1 GHz. (b) The same resonator as K2 at 6 GHz with unmatched 1-mm loop transducer. We see that the S_{11} notch does not coincide with the S_{21} peak and the insertion loss is higher. Moreover the off-resonance rejection is also lower than in (a).

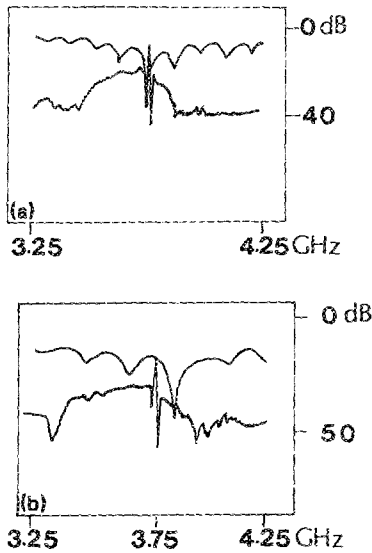


FIG. 4. (a) Shows the resonator response with the resonator X1 and 1-mm matched transducer at 3.75 GHz. Insertion loss close to 7 dB had been achieved. The S_{21} peak coincides with S_{11} peak as is expected for good matching. Before matching the latter was occurring at 83 MHz higher [part (b)]. Matching improved the insertion loss in this case by 8 dB. (b) Shows the same resonator response with an unmatched transducer. As before we see that the S_{11} notch does not coincide with the S_{21} peak B.

$$\epsilon_{\text{eff}}^L = \frac{\epsilon_r + 1}{2} \left[1 + \frac{29.98}{Z_{0L}} \left(\frac{2}{\epsilon_r} + 1 \right)^{0.5} \times \frac{\epsilon_r - 1}{\epsilon_r + 1} \left(\ln \frac{\pi}{2} + \frac{1}{\epsilon_r} \ln \frac{4}{\pi} \right)^2 \right], \quad (3)$$

for $Z_{0L} > 50 \Omega$, i.e., for inductive microstrip, ϵ_r for quartz = 3.8, and $\epsilon_{\text{eff}}(L)$ for inductor microstrip AB ($Z_{0L} = 100 \Omega$) can be obtained from Eq. (3). ϵ_{eff} for capacitance microstrip can be determined by first finding out Z_{0c} corre-

sponding to the microstrip of width $W_2 \cong 0.55$ mm from the following equations:

$$W/h_s = [\exp(H')/8 - \frac{1}{4} \exp(H')]^{-1},$$

where

$$H' = Z_{0c} [2(\epsilon_r + 1)]^{0.5}/119.9 + \frac{0.5(\epsilon_r - 1)}{\epsilon_r + 1} \left(\ln \frac{\pi}{2} + \frac{1}{\epsilon_r} \ln \frac{4}{\pi} \right). \quad (4)$$

$h_s = 250 \mu\text{m}$ is the quartz substrate thickness and Z_{0c} is then used in Eq. (2) to determine ϵ_{eff} . Now the frequency dependence of $\epsilon_{\text{eff}}(L, C)$ was taken into consideration. ϵ_{eff} ($f = 4.5$ GHz) is determined for corresponding Z_{0L} and Z_{0c} from Eqs. (2) and (3) with the help of Eq. (1). $\lambda_g(C)$ and $\lambda_g(L)$ can then be determined from the equation

$$\lambda_g(L, C) = 300/f [\epsilon_{\text{eff}}(L, C) (f = 4.5 \text{ GHz})]^{0.5}$$

using corresponding ϵ_{eff} as obtained above.

As applicable to the microstrips and the equivalent circuits (Fig. 1) the following expressions allow us a unique determination of the required length l_i of the inductor microstrip. It was assumed that $L_1 = L_2$, then we have the following equations:

$$2L_1 + L_3 = 1.51 \text{ nH},$$

$$C + 2C_L = 0.3 \text{ pF},$$

$$L_1 = l_c Z_{0c} / 2 f \lambda_{gc},$$

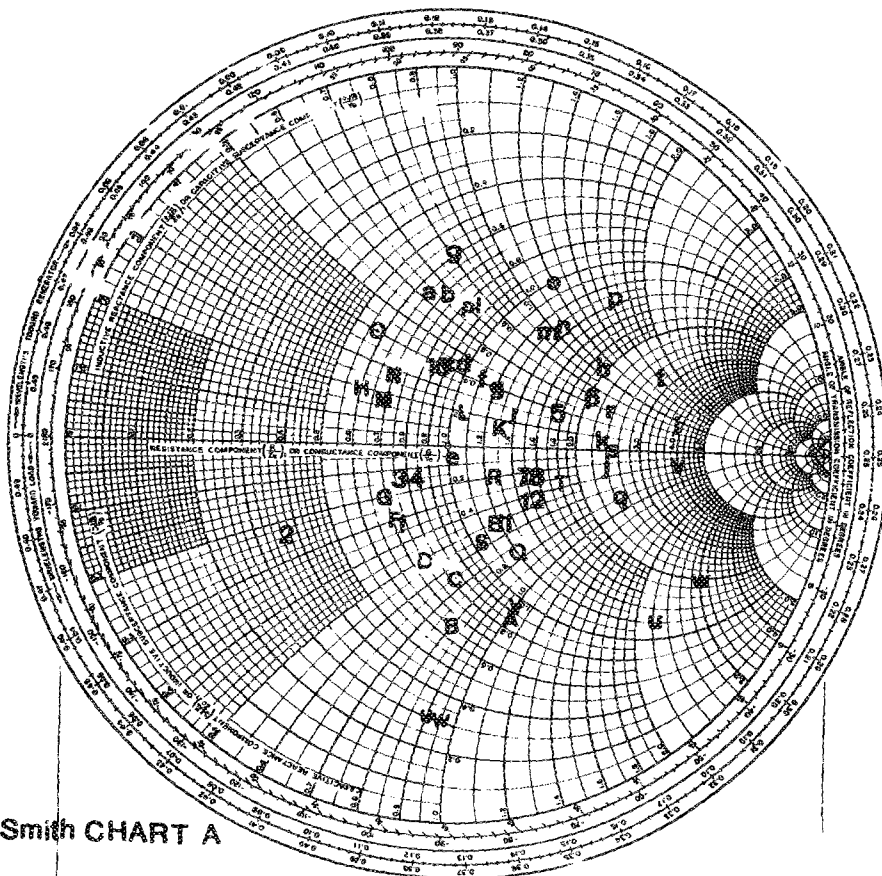


FIG. 5. Measured S_{11} parameters for the resonator I ($7\text{-}\mu\text{m}$ YIG film) with 1-mm unmatched transducer are shown in alphabetic orders denoted by small letters at frequencies: 3.0, 3.2, 3.4, 3.6, 3.8, 4.0, 4.2, 4.4, 4.6, 4.8, 5.0, 5.1, 5.2, 5.3, 5.4, 5.5, 5.55, 5.65, 5.75, 5.85, 5.95, and 6.0 GHz. Capital letters show measured S_{11} at above frequencies with matched transducer. Numbers show S_{11} measured with another resonator (K2) built with $14\text{-}\mu\text{m}$ YIG film, with matched transducer in the range 3–6 GHz at steps of 0.2 GHz.

$$C = l_c / f \lambda_{gc} Z_{oc},$$

$$C_L = l_l / 2 f Z_{oL} \lambda_{gL},$$

$$l_l = (\lambda_{gL} / 2\pi) \sin^{-1}(\omega L_s / Z_{oL}).$$

Z_{oc} was used in the above equations as an unknown parameter, rather than the characteristic impedance of the 5-mm microstrip between B and A in Fig. 2. (At A and B there are microstrips of different characteristic impedances.) Next the width W of the inductor microstrip between B and C [Fig. 2(b)] was determined from¹⁰

$$Z_{oL} = \frac{119.9}{[2(\epsilon_r + 1)]^{0.5}} \left[\ln \left\{ \frac{4h_s}{w} + \left[16 \left(\frac{h_s}{w} \right)^2 + 2 \right]^{0.5} \right\} - 0.5 \left(\frac{\epsilon_r - 1}{\epsilon_r + 1} \right) \frac{\ln \pi}{2} + \frac{1}{\epsilon_r} \ln \frac{4}{\pi} \right],$$

where $h_s = 0.25$ mm is the substrate thickness.

Final length l_l and the width W of the inductor microstrip were calculated to be 1.1 mm and 131 μ m. The matched transducer we then fabricated through the usual photolithographic technique. The output transducer was a mirror image of the input transducer shown in Fig. 2. After matching the following improvements have been observed.

RESULTS OF TRANSDUCER MATCHING

(1) It has been possible to reduce the insertion loss by 6 dB more, i.e., the insertion loss at resonance with most of the 1-mm resonators can be kept at 6–14 dB over 3 GHz; the insertion loss as low as 6 dB at resonance has been obtained for some resonators (Fig. 4). Relative improvements at matching can be seen in Figs. 3(a), (b) and 4(a), (b). After matching we see that the S_{21} peak coincides with the S_{11} notch which results in reduced IL. The lowest IL achieved with a 1-mm matched transducer was 13 dB at 6 GHz with the resonator K2 (Table II).

(2) The out off-resonance rejection has been improved

by 4 dB, i.e., 10–14 dB within 3–6 GHz. Before matching it was around 7–10 dB. The maximum out off-resonance rejection achieved with resonator K2 was more than 15 dB.

(3) The S_{11} parameters measured with a matched transducer have been found to be quite low (0.15) around 5–6 GHz when compared to those of the computer optimized values (see Smith chart A in Fig. 5). This is also reflected in the coincidence of reflection notch with resonance peak S_{21} (Figs. 3 and 4).

(4) Tunability also improved significantly after matching. The resonators were tunable well beyond 6 GHz with minimum resonance rejection of 10 dB throughout the range (i.e., without the need of any tweaking).

With most of the resonators, matched transducers did not provide higher Q resonance.

ACKNOWLEDGMENTS

The author thankfully acknowledges financial support and guidance given by Professor J. M. Owens. The author is also grateful to Professor R. L. Carter for encouragement and helpful suggestions during the progress of the work.

¹M. S. Sodha and N. C. Srivastava, *Microwave Propagation in Ferrimagnetics* (Plenum, New York, 1981), p. 170.

²L. K. Brundle, *Electron Lett.* **4**, 132 (1968).

³W. R. Brinlee, J. M. Owens, C. V. Smith, Jr., and R. L. Carter, *J. Appl. Phys.* **52**, 2276 (1981).

⁴J. P. Castera, *Proceedings of the RADC Workshop, Rome*, 10–11 June, 1981, p. 218.

⁵J. H. Collins, J. D. Adam, and Z. M. Bardai, *Proc. IEEE* **65**, 1090 (1977).

⁶E. P. Snapka, M. S. thesis, The University of Texas at Arlington, Arlington, TX, May 1978.

⁷K. W. Reed, A. K. Reddy, and W. A. Davis, *Intl. Microwave Symp. Digest, IEEE MTT 519* (1985).

⁸E. Huijter and W. Ishak, *IEEE Trans. Mag.* **MAG-20**, 1232 (1984).

⁹D. K. De, *J. Appl. Phys.* **64**, 2144 (1988).

¹⁰*Foundations for Microstrip Circuit Design*, edited by T. C. Edwards (Wiley, London, 1981), p. 216.